

AFFORDABLE FABRICATION AND PROPERTIES OF SILICON CARBIDE-BASED INTERPENETRATING PHASE COMPOSITES

10-24
372/22

Mrityunjay SINGH

FDC-NYMA, Inc., MS 106-5, NASA Lewis Research Center Group, Cleveland, OH
44135 (USA)

An affordable processing technique for the fabrication of silicon carbide-based interpenetrating phase composites (IPCs) is presented. This process consists of the production of microporous carbon preforms and subsequent infiltration with liquid silicon or silicon-refractory metal alloys. The microporous preforms are made by the pyrolysis of a polymerized resin mixture for which methods to control pore volume and pore size have been established. The process gives good control of microstructure and morphology of silicon carbide-based composite materials. Room and high temperature mechanical properties (flexural strength, compressive strength, and flexural creep) of low and high silicon-silicon carbide composites will be discussed.

1. INTRODUCTION

Silicon carbide-based ceramic and composite materials have good strength, high thermal conductivity, and good creep and environmental resistance at high temperatures [1]. These attractive thermomechanical properties have led to their use in a number of applications in aeronautics, energy, process, electronic and nuclear industries. In the aeronautical arena, composite materials are being considered for applications in jet engine components. Applications in the energy industries include radiant heater tubes, heat exchangers, heat recuperators, and components for land based turbines for power generation. These materials are also being considered for use in the first wall and blanket components of fusion reactors, in furnace linings, and bricks, and in components for diffusion furniture (boats, tubes) in the microelectronics industry.

There are a number of critical issues related to commercially available silicon carbide-based ceramic materials. The majority of these materials are fabricated by a reaction bonding process which typically consists of molten silicon infiltration into silicon carbide and carbon containing green bodies or preforms. The resulting materials, also referred to as reaction bonded silicon carbide (RBSC), contain silicon carbide grains bonded together by a silicon phase. There is a wide variation in the microstructural features of

final materials e.g., interconnectivity of the silicon carbide network, and the morphology and amount of the silicon phase. These features are detrimental to high temperature thermomechanical properties, and limit the temperature capability of these materials.

Some of these issues can be addressed by using silicon carbide-based interpenetrating phase composites in which the silicon carbide phase forms a continuous interpenetrating network through the body with good control over the interconnectivity of the second phase. In an extensive review, Clarke [2] has discussed various design philosophies and processing approaches for interpenetrating phase composites. These materials have a three dimensional microstructure with multifunctional characteristics. A number of silicon carbide-based interpenetrating phase composites (IPCs) have been produced by reactive infiltration of interconnected porous carbon preforms [3-6]. These preforms have been fabricated by the phase separation and pyrolysis process [3-10]. This is a low cost processing technique which requires fabrication times and/or temperatures significantly lower than other conventional processing techniques. The materials produced are fully dense, with excellent control of the primary phase microstructure, the amount and distribution of second phases, and the detrimental effects of sintering aids are avoided [11-23].

The overall objective of this program is to develop and fabricate affordable silicon carbide-based IPC materials with tailorable microstructure and thermomechanical properties. In this paper, the fabrication approach, microstructure, and mechanical properties (flexural strength, compressive strength, and flexural creep) of a wide variety of silicon carbide-based interpenetrating phase composites will be presented.

2. EXPERIMENTAL PROCEDURES

A schematic description of the fabrication process is given in Fig. 1. This process consists of the production of a microporous carbon preform [7-10] and its subsequent infiltration with liquid silicon or silicon-refractory metal alloys. The microporous preforms are made by the pyrolysis of a polymerized resin mixture with good control of pore volume and pore size. During the polymerization process, phase separation of the resin and pore former takes place. The pore volume and pore size can be controlled by changing the amount and type of pore formers, curing time, and temperature [8-9]. The interconnectivity of the porous network is critical in achieving the desired properties in the composites.

The silicon carbide-based interpenetrating phase composites (IPCs) produced by this process demonstrate a high degree of control over the primary phase morphology and the

amount and distribution of second phases. Materials with variable volume percent of silicon can be produced within a continuous network of silicon carbide. The nature and amount of second phases can be controlled by proper selection of infiltrants and infiltration conditions.

Microstructures of the microporous preforms used for the fabrication of silicon carbide-based composites are shown in Fig. 2 (a) and (b). Mercury porosimetry data on these preforms indicate that virtually all the porosity is open to infiltration. All the composite materials used in this study were fabricated by the reactive infiltration of molten silicon into these preforms. The details of carbon preform fabrication [8-9] and other infiltration conditions have been described elsewhere [4-5]. The control of processing conditions is critical to avoid microstructural coarsening, silicon vein and lake formations, and cracking due to thermal expansion mismatch and volume change. After infiltration, samples were cross-sectioned and polished for metallographic studies. Powder x-ray diffraction analyses was used to identify different phases in these materials.

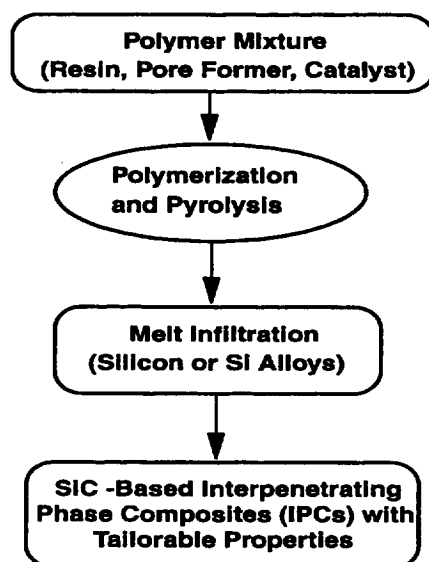


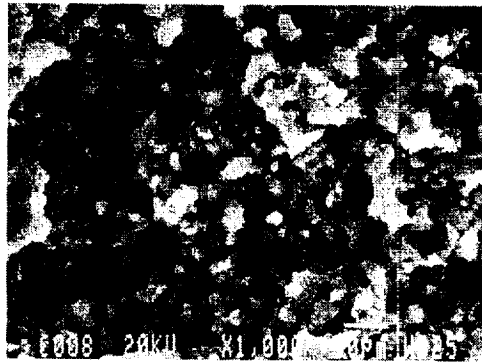
Fig. 1: Process flow chart for the fabrication of silicon carbide-based materials.

Flexural specimens measured 50 mm long, 4 mm wide and 3 mm thick. Four point flexural testing was carried out per MIL-STD-1942 (MR) using configuration B specimens with 20 mm inner and 40 mm outer spans, and a loading rate of 0.5 mm/min [16-19]. At least, six to ten specimens were tested at room temperature and five specimens were tested in air at each high temperature. However, in the case of NC-430 only two samples were tested at each temperature and the data represents the average strength. After flexure testing, fracture surfaces were examined in optical and scanning electron microscopes to identify the failure origins.

For the compression test, rectangular samples 2.3 x 2.3 x 4 mm were used. The specimens were tested in compression at a constant strain rate of $2 \times 10^{-5} \text{ s}^{-1}$ at temperatures ranging from 1250 to 1450 °C in air. Further details of the test conditions are discussed in other publications [23-24].



(a)



(b)

Fig. 2: Microstructures of porous carbon preforms used for composite fabrication.

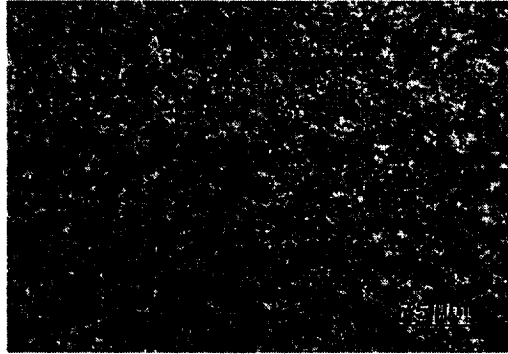
Flexural creep tests [22] were conducted with a lever arm machine (Applied Test Systems, Butler, PA) using a silicon carbide four-point bend fixture. The displacement was measured using an LVDT with a three-point extensometer made of alumina gage rods with silicon carbide tips. The silicon carbide tips were in contact with the specimen tensile surface at the center and beneath the inner load points. Relative deflection was recorded by a data acquisition system. After creep experiments, the tensile and compression sides of the crept specimens were examined in SEM.

3. RESULTS AND DISCUSSION

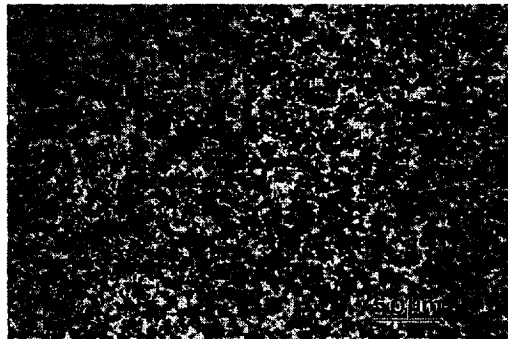
3.1 Microstructure

Optical micrographs of two types of silicon carbide composite materials, designated as low silicon (LSSC) and high silicon (HSSC), are shown in Fig. 3 (a) and (b). These

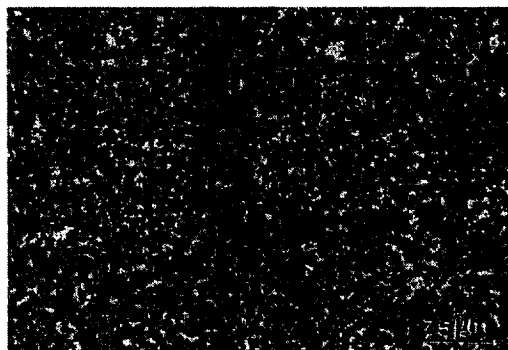
microstructures indicate the uniform distribution of silicon phase (white) throughout a silicon carbide matrix (gray). The silicon contents of low and high silicon composites, shown in Fig. 3 (a) and (b), were estimated to be ~14-16 % and ~24-26% by x-ray diffraction and image analyses. For comparison, the microstructure of a reaction bonded silicon carbide (REFEL-SiC) is shown in Fig. 3 (c). This material has a silicon content similar to the low silicon-silicon carbide composite (LSSC), but its fabrication route is different (reaction bonding of SiC grains).



(a)



(b)



(c)

Fig. 3: Microstructure of silicon carbide-silicon composites (a) low silicon (LSSC), (b) high silicon (HSSC), and (c) REFEL reaction bonded silicon carbide (Si is white and SiC is gray).

3.2 FLEXURAL STRENGTH

The flexural strengths of low silicon-silicon carbide composite (LSSC) material along with two types of commercial silicon carbides at different temperatures are given in Table 1. The average room temperature strength of this composite material is 371 ± 28 MPa. The data represents mean results for ten tests at room temperature and five tests at elevated temperatures. In general, flexural strengths of LSSC are higher than the two commercial silicon carbides. At 1371°C , the flexural strength of NC-433 reaction bonded silicon carbide decreases $\sim 20\%$ while there is no strength loss in low silicon-silicon carbide composite (LSSC) materials. The apparent increase in strength of all the specimens at 1100°C may be due to silica formation and healing of machining damage. Further experimental studies are in progress to confirm this phenomena.

Table. 1: Flexural Strength of low silicon-silicon carbide composite (LSC) and commercial silicon carbide materials.

Test Temperature ($^{\circ}\text{C}$)	Flexural Strength (MPa)		
	LSSC	NC 433	NC430
25	371 ± 28	253 ± 26	146
1100	545 ± 31	274 ± 15	150
1260	422 ± 35	295 ± 15	187
1371	395 ± 30	200 ± 23	167

3.3 COMPRESSIVE STRENGTH

The stress-strain curve of constant strain rate experiments for low and high silicon-silicon carbide composites (LSSC and HSSC) and for REFEL reaction bonded silicon carbide, are shown in Fig. 4. The experiments were stopped when the stress on the sample started to decrease. This occurred at strains of 4 to 17 %. The strains at which the decrease in strength initiates are considerably larger at lower temperatures. The deformed samples showed microcracking, but catastrophic crack propagation did not occur. The compressive strength of low silicon-silicon carbide composite (LSSC) was considerably higher than the strength of REFEL reaction bonded silicon carbide material although both materials had quite similar silicon contents. In addition, the compressive strength of LSSC are also higher than high silicon-silicon carbide composites (HSSC).

The stress-strain curves for composites in Fig. 4 show three regions: a linear elastic region, a non stationary region of plastic deformation where a continuous increase of stress is necessary in order to advance the deformation of the material at the strain rate imposed by the experiment, and a third region in which the material accommodates plastic deformation by formation and coalescence of cavities with a subsequent decrease in strength.

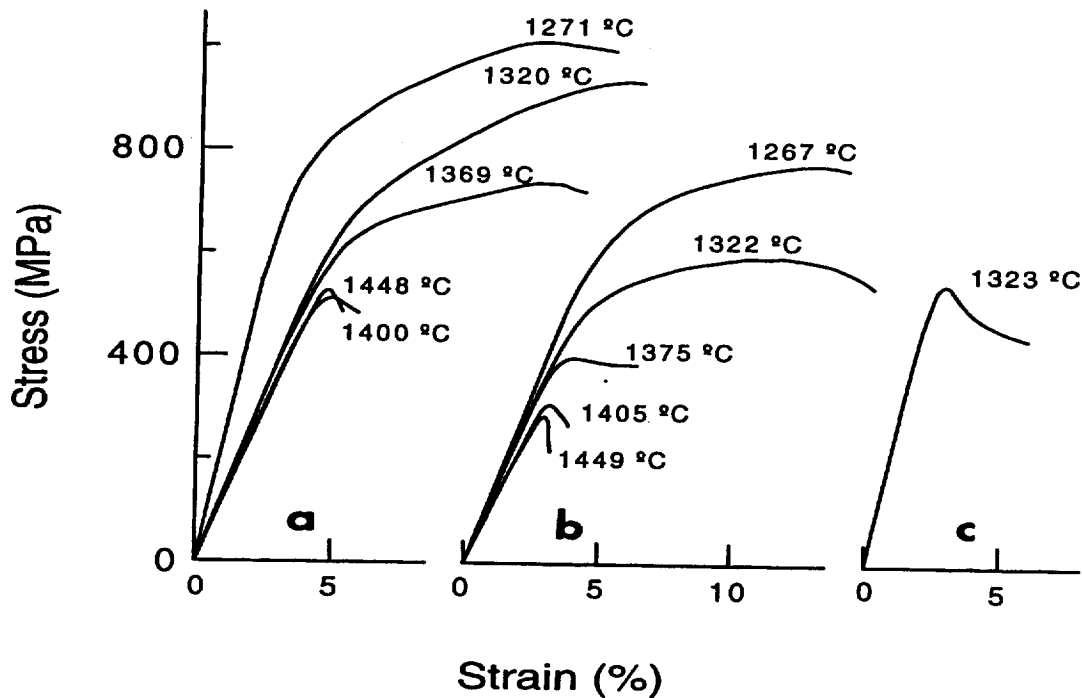


Fig. 4: Plot of compressive stress versus strain for (a) low silicon-silicon carbide composite (LSSC), (b) high silicon-silicon carbide composite (HSSC), and (c) REFEL-reaction bonded silicon carbide at high temperatures.

Both silicon carbide interpenetrating phase composites (LSSC and HSSC) used in this study are composed of a continuous silicon carbide (SiC) network with silicon filling the pores. This microstructure cannot be deformed without the deformation of both components, so the total strength and plastic deformation have contributions of all the phases present. The lower strength of the HSSC over the LSSC material at all temperatures (in Fig. 4), is related to the lower amount of SiC present (attributed to different initial carbon preform density), indicating clearly that the strength is dominated by the silicon carbide network. It is important to point out the high deformation resistance of the LSSC material, which reaches a value of 500 MPa at temperatures over the

melting point of silicon (Fig. 4), will only be possible when the interpenetrating silicon carbide network is bearing the load. The compressive strength of REFEL reaction bonded silicon carbide is lower than low silicon-silicon carbide composite material (LSSC) due to absence of continuous silicon carbide network and accelerated deformation of silicon which is used as reaction bonding phase.

3.4 FLEXURAL CREEP

Creep strain vs time plots for three temperatures at different flexural stresses were generated. Final percent strain was calculated from measurements made on unfailed test bars. The creep rates and calculated strains are given in Table 2. The comparison of creep rates of the low silicon-silicon carbide composite (LSSC) with literature data indicate that the flexural creep resistance of this material is higher than that of most reaction-bonded silicon carbide materials [24].

Table 2: Status at 100 hrs. for flexural creep tests on low silicon-silicon carbide composite (LSSC).

Temperature, °C	Stress (MPa)	Creep rate (s ⁻¹)	Creep strain (%)
1200	200	1.34 x10 ⁻⁹	0.13
1260	200	2.59 x10 ⁻⁹	0.18
1320	200	7.8 x10 ⁻⁹	0.30
1320	150	4.43 x10 ⁻⁹	0.29

The post-test examination of bars revealed the presence of cracks in the surface silica layers. The microstructures of compression and tension regions were studied in order to gain insight into the creep mechanism. The scanning electron micrographs of regions under compressive and tensile stresses show significant differences. There were more silicon precipitates on the tensile side of the specimens than on the compression side. The tensile side had more cavities than the compression side. These cavities primarily formed at multiple grain junctions in preference to grain boundaries. The preliminary microscopic data indicate a mechanism of cavitation during creep [22]. The detailed TEM analysis of crept specimens is underway and will be reported elsewhere.

4. CONCLUSIONS

The findings of this work suggest that the reaction forming process can be used to fabricate silicon carbide-based interpenetrating phase composite materials with tailorable properties. The materials produced by this process are fully dense, with excellent control of microstructure, second phases, and eliminate the detrimental effects of sintering aids. These materials have superior high temperature flexural strength, compressive strength, and creep properties compared to most reaction bonded silicon carbide materials. The high temperature mechanical properties of composites can be controlled by controlling the pore volume fraction within the carbon preforms, thus controlling the volume fraction of the silicon carbide network in the interpenetrating phase composite body.

REFERENCES

- 1) D.C. LARSEN, J. ADAMS, L. JOHNSON, A. TEOTIA, and L. HILL, "Ceramic Materials for Heat Engines", Noyes Publications, NJ (1985).
- 2) D.R. CLARKE, J. Am. Ceram. Soc., 75, 4 (1992) 739-759.
- 3) E.E. HUCKE, AMMRC Report TR-83-5, January 1983.
- 4) M. SINGH and S.R. LEVINE, NASA TM -107001 (1995).
- 5) M. SINGH, in 'Progress in Thermal Treatment of Materials', Ed. P. Ramakrishnan, New Age International (P) Limited, Publishers, (1996) 41-52.
- 6) Y-M. CHIANG, R.P. MESSNER, C. TERWILLIGER, and D.R. BEHRENDT, Mater. Sci. Engg. A 144, (1991) 63-74.
- 7) S.K. DATTA, N. SIMHAI, S.N. TEWARI, J.E. GATICA, and M. SINGH, Metall. and Mater. Trans. A, 27A, 11 (1996) 3669-3674.
- 8) M. SINGH and R.F. DACEK, in 'Microporous and Macroporous Materials', MRS Symp. Proc., Vol. 431, Materials Research Society, Warrendale, PA (1996) 403-407.
- 9) M. SINGH and S.C. FARMER, J. Mater. Sci. Letters, 16 (1997) 946-949.
- 10) K.P. CONSTANT, J-R. LEE, Y-M. CHIANG, J. Mater. Res., 11, 9 (1996) 2338-2345.
- 11) M. SINGH, D.R. BEHRENDT, and R.F. DACEK, NASA CP-3175 (1992) 695-705.
- 12) M. SINGH and D.R. BEHRENDT, NASA TM-105860 (1992).
- 13) M. SINGH and D.R. BEHRENDT, NASA TM-106414 (1993).
- 14) M. SINGH and D.R. BEHRENDT, J. Mater. Synth. and Process., 2, 2 (1994) 133-139.
- 15) M. SINGH and T.A. LEONHARDT, Microstructural Charact., 35, 4 (1995) 221-228.
- 16) M. SINGH, R. PAWLIK, J.A. SALEM and D.R. BEHRENDT, in 'Advances in Ceramic Matrix Composites', American Ceramic Society, Westerville, Ohio (1993) 349-360.

- 17) M. SINGH and D.R. BEHRENDT, Mater. Sci. Engg., A187 (1994) 183-187.
- 18) M. SINGH and D.R. BEHRENDT, J. Mater. Res., 9, 7 (1994) 1701-1708.
- 19) M. SINGH and D.R. BEHRENDT, Mater. Sci. Engg., A194 (1995) 193-200.
- 20) A. WOLFENDEN, P.J. RYNN and M. SINGH, J. Mater. Sci., 30 (1995) 5502-5507.
- 21) A. WOLFENDEN, K.A. OLIVER and M. SINGH, J. Mater. Sci., 31(1996) 6073-6076.
- 22) M. SINGH and W.A. SANDERS, Ceram. Engg. and Sci. Proc., 16, 4 (1995) 113-120.
- 23) A. MUNOZ, J. MARTINEZ-FERNANDEZ, A. DOMINGUEZ-RODRIGUEZ and M. SINGH, J. Eur. Ceram. Soc., 18 (1998) 65-68.
- 24) J. MARTINEZ-FERNANDEZ, A. MUNOZ, A. DOMINGUEZ-RODRIGUEZ and M. SINGH, World Ceramics Congress Proceedings, Italy (1998).